Supporting Information

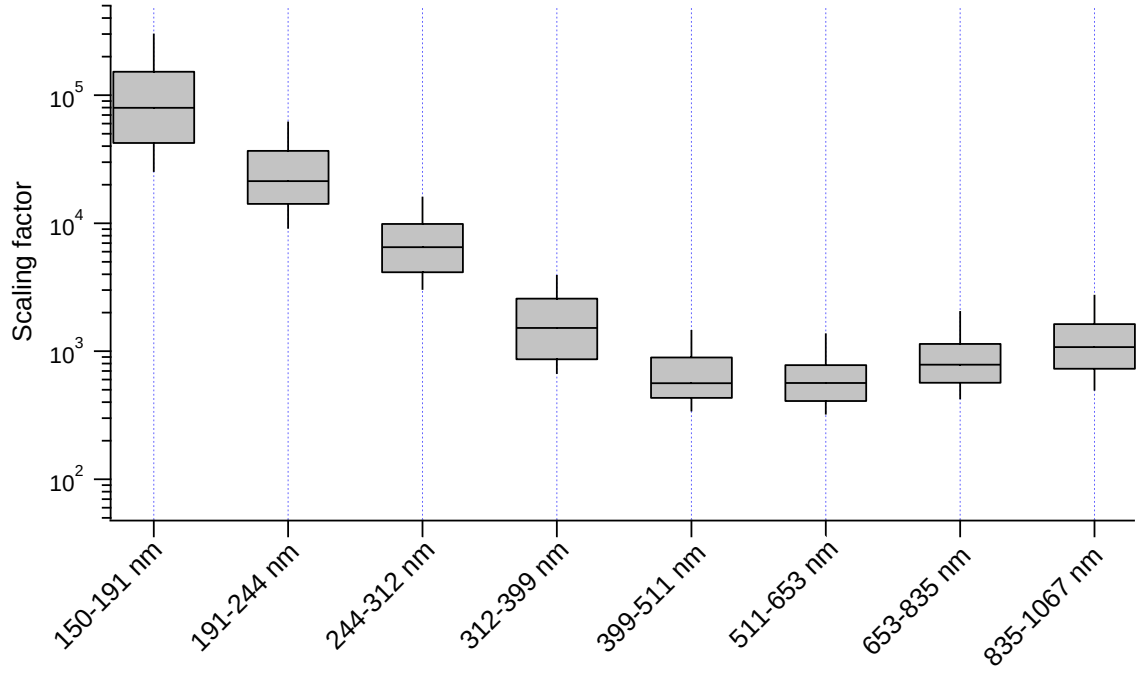

Fig. S1: Box-plot of hourly size-dependent scaling factors for the entire measurement period (n = 624). Median, 75th percentile and 90th percentile are denoted by the solid line, box and whisker respectively.

The scaling factors employed here were observed to be strongly dependent upon particle size, but the magnitude of the factors is similar to that observed in previous studies involving the use of laser particle counters, aerodynamic particle sizers and scanning mobility particle sizers to scale ATOFMS particle number concentrations (Wenzel et al., 2003; Qin et al., 2006; Pratt et al., 2009). The size bin width was generated by merging adjacent pairs of TDMPS size bins because the original size bins were found to be too narrow, resulting in low ATOFMS hourly counts in some bins during certain periods of the measurement campaign. The uncertainty associated with the TDMPS particle number concentrations in the size range used here (100-712 nm, mobility diameter) is estimated to be < 2% (Birmili et al., 1999). The bins used are wider than those used previously by Pratt et al (2009) but narrower than those

used by Wenzel et al (2003) and Qin et al (2006). The bin width was not increased any further because, although this would reduce the magnitude of the scaling factors required, information on the size-dependence of the elemental carbon particle mass associated with different sources would be lost.

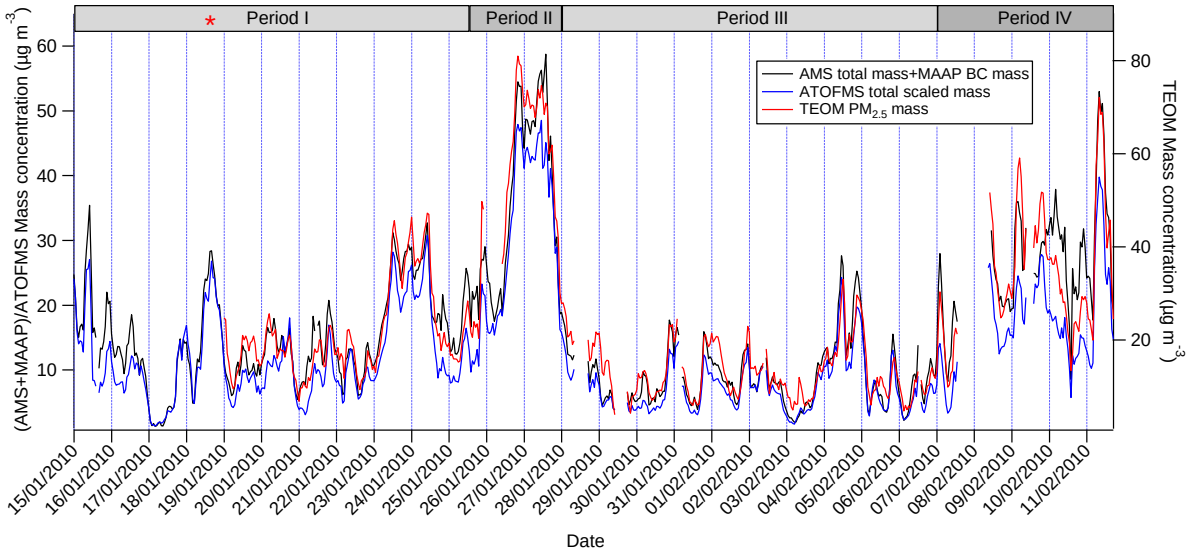

Fig. S2: ATOFMS total scaled particle mass concentration (150-1067 nm, d_{va}), sum of AMS total mass (ammonium + chloride + nitrate + sulfate + organics) + MAAP BC mass concentration, and TEOM $PM_{2.5}$ mass concentration.

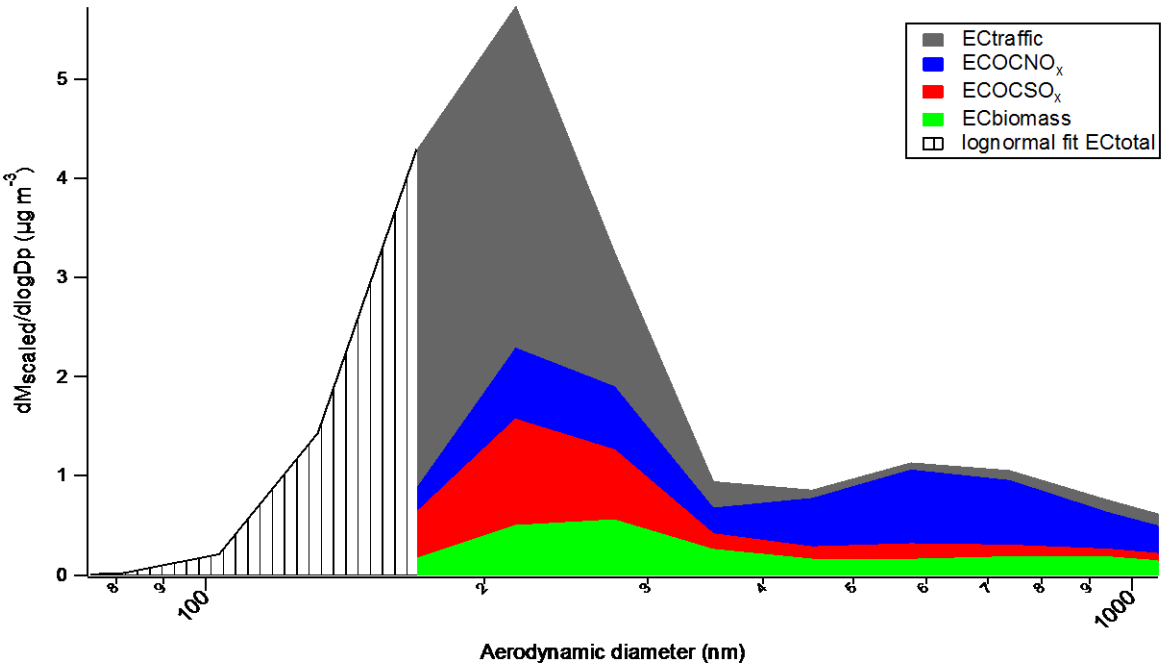

Fig. S3: Lognormal fit of the average scaled ATOFMS mass size distribution for EC particles extrapolated below 150 nm. Only the the size bins covering the size range of the smaller mode (150-400 nm) were used to generate the lognormal curve. The mass contribution below 150 nm is ~9% of the total.

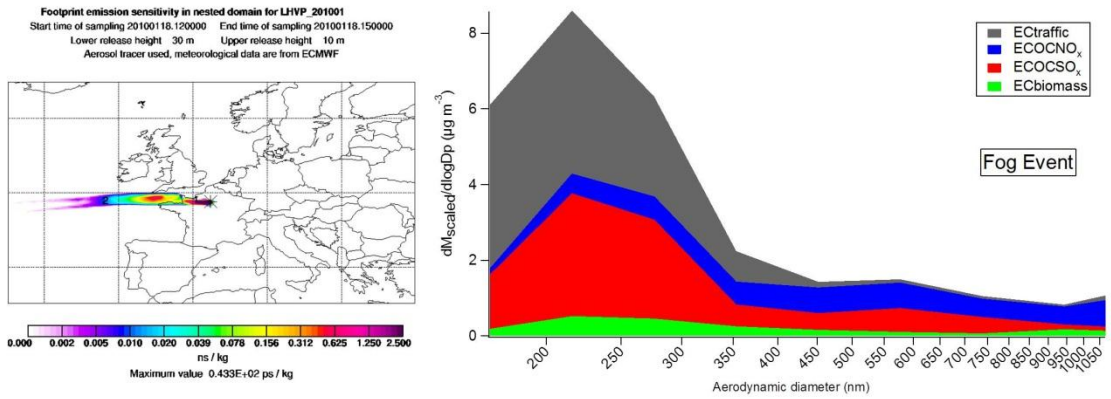

Fig. S4: Potential emission sensitivity (left) and average mass size distribution for the 4 ATOFMS EC classes (right) on 18/01/2010. The numbers in the potential emission sensitivity plots correspond to the air mass age in days, and are positioned on the centroid of the retroplume position at that time.

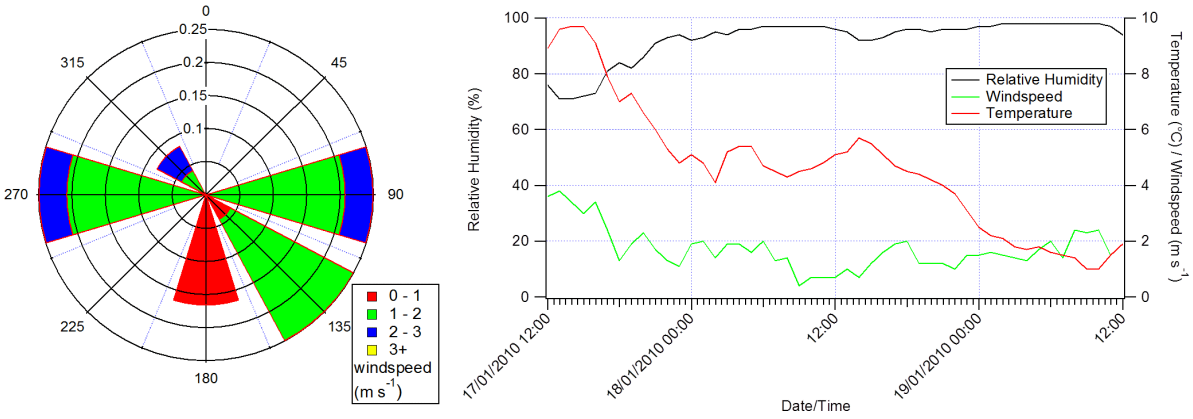

Fig. S5: Windrose for 18/01/2010 (left) and meteorological data for the period of interest (right). Meteorological data provided by Meteo France, Parc Montsouris, (48°49'18N. 2°20'12E. 75m a.s.l.), approximately 1.5 km from LHVP.

Fig. S6: Photograph taken at LHVP at 11:30 on 18/01/2010

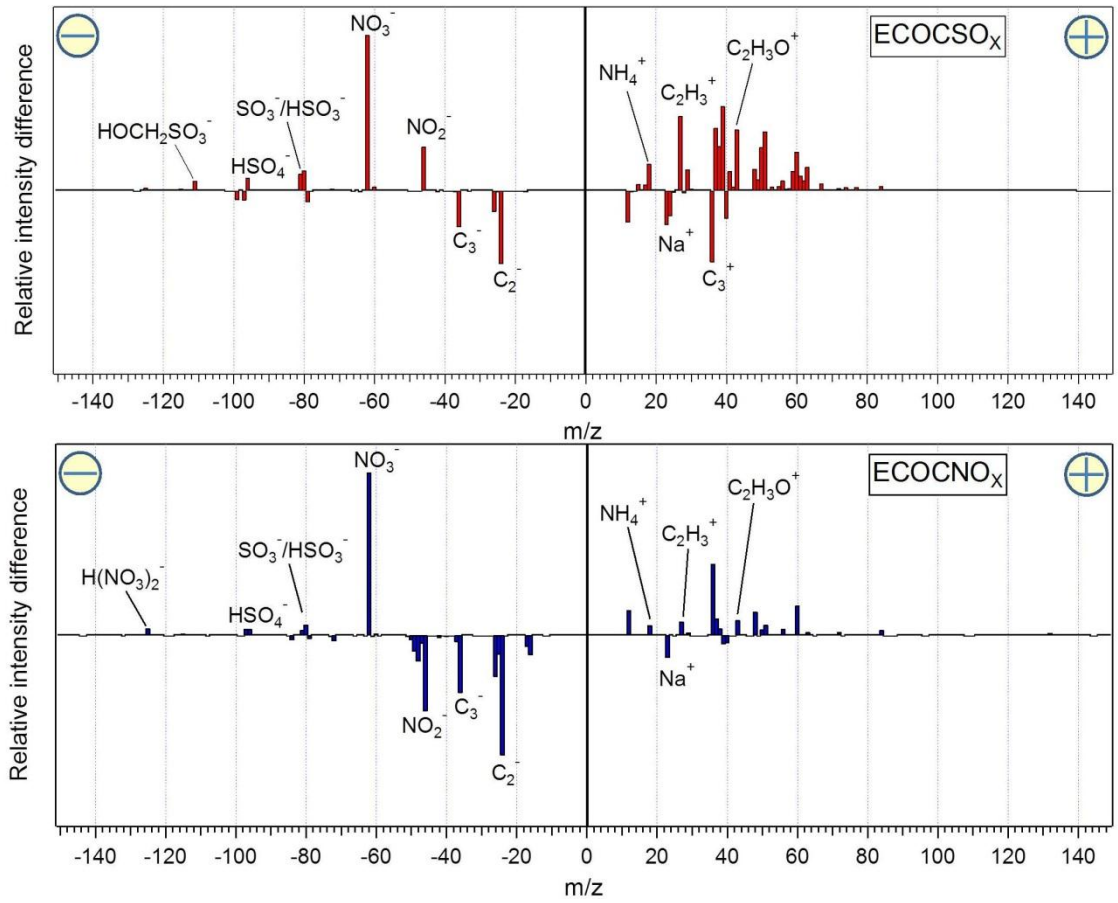

Fig. S7: Difference mass spectra for ECOCSO$_x$ (top) and ECOCNO$_x$ (bottom) particles below and above 400 nm (d_a) on 18/01/2010. Relative intensity difference above the line indicates enhancement of these species in the larger particles.

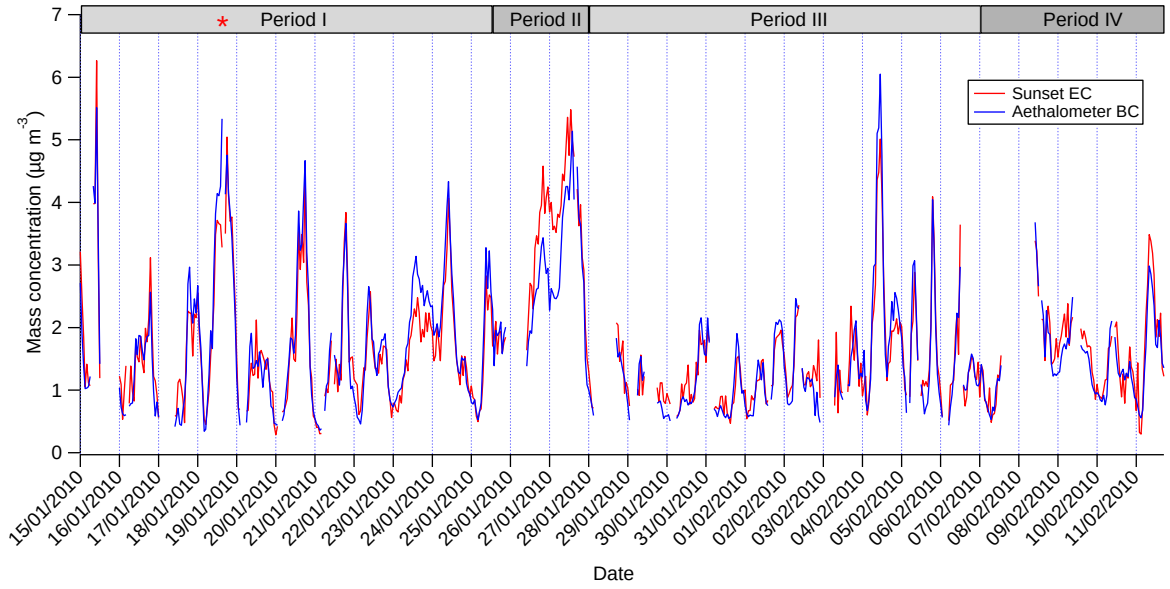

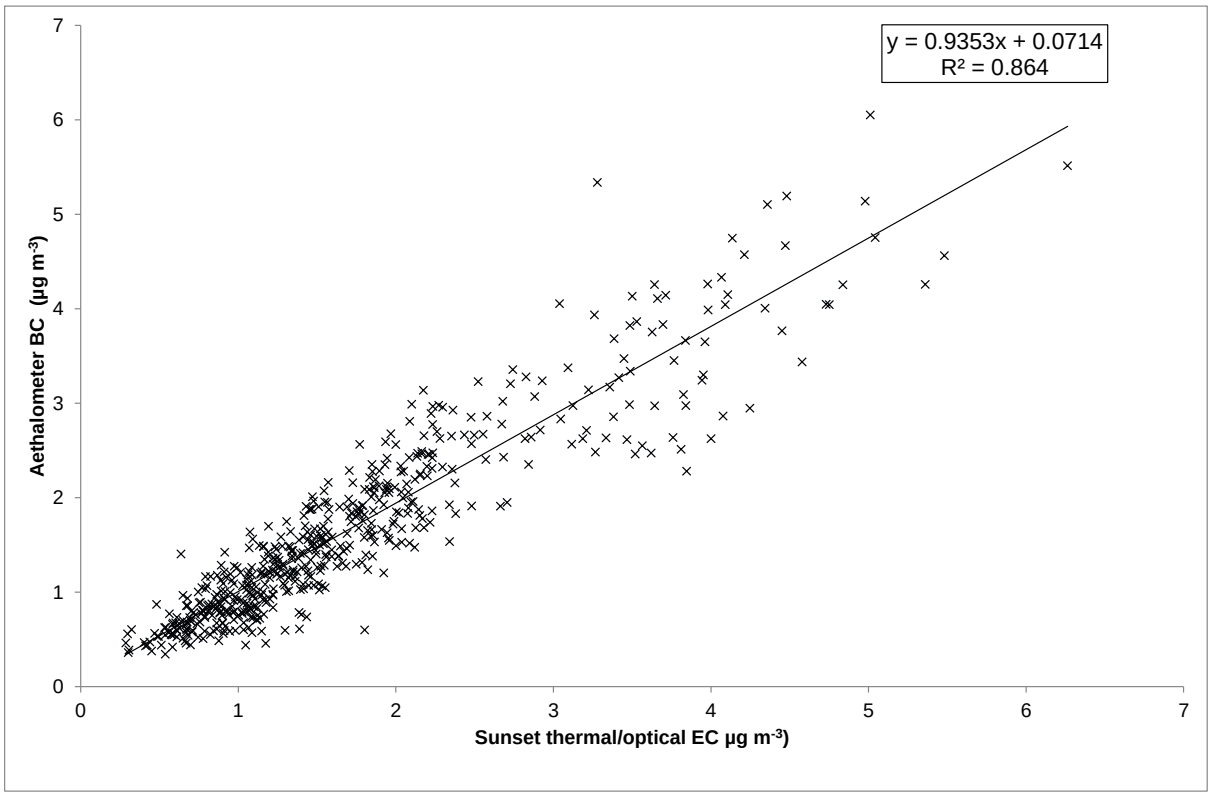

Fig. S8: Comparison of Sunset analyzer thermal/optical EC and aethalometer BC

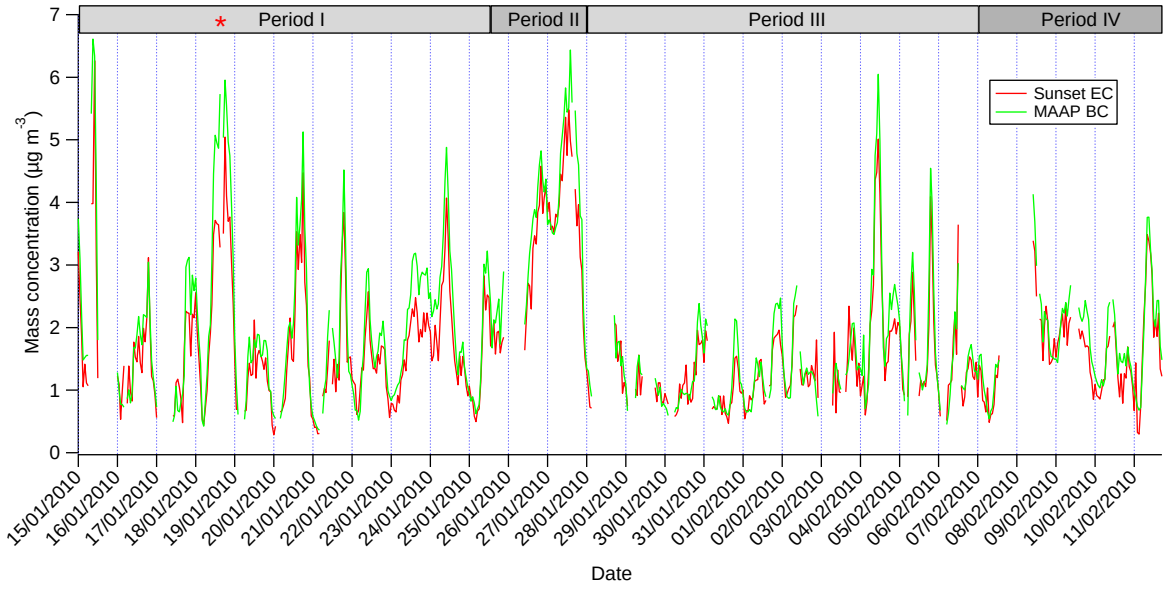

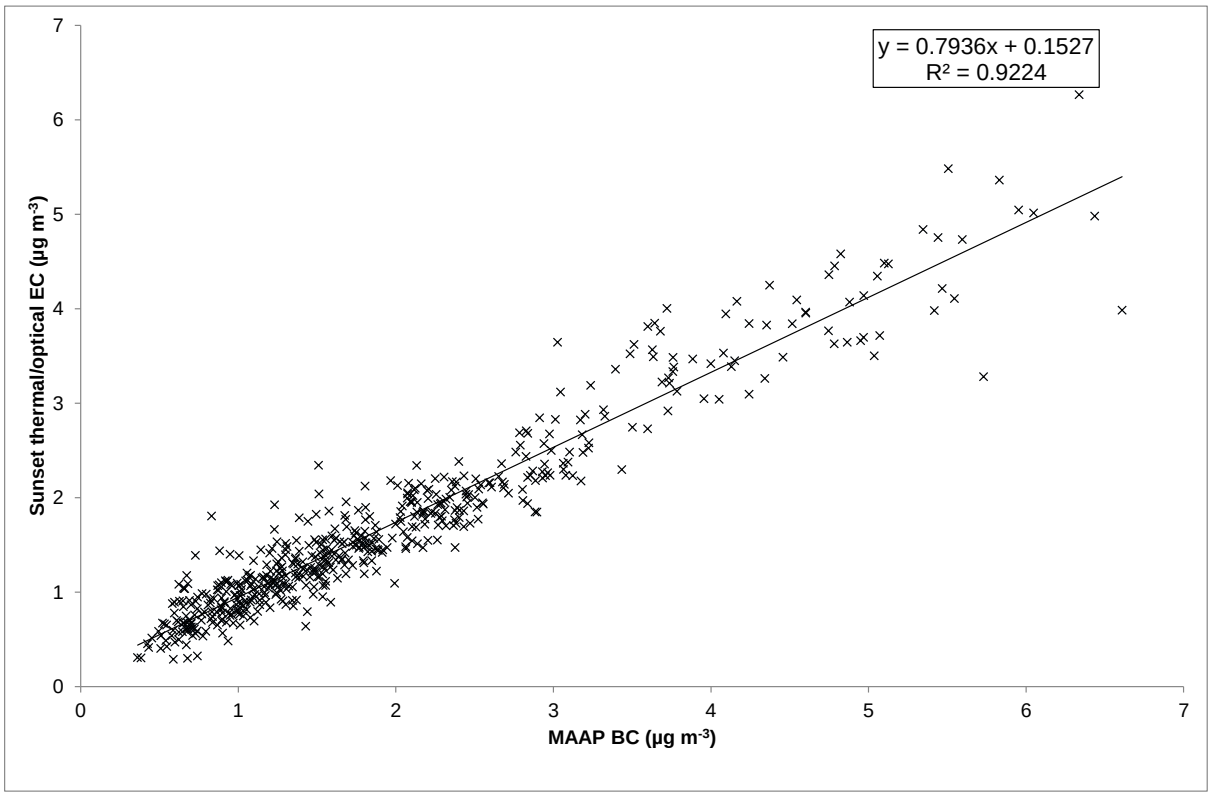

Fig. S9: Comparison of Sunset thermal/optical EC and MAAP BC

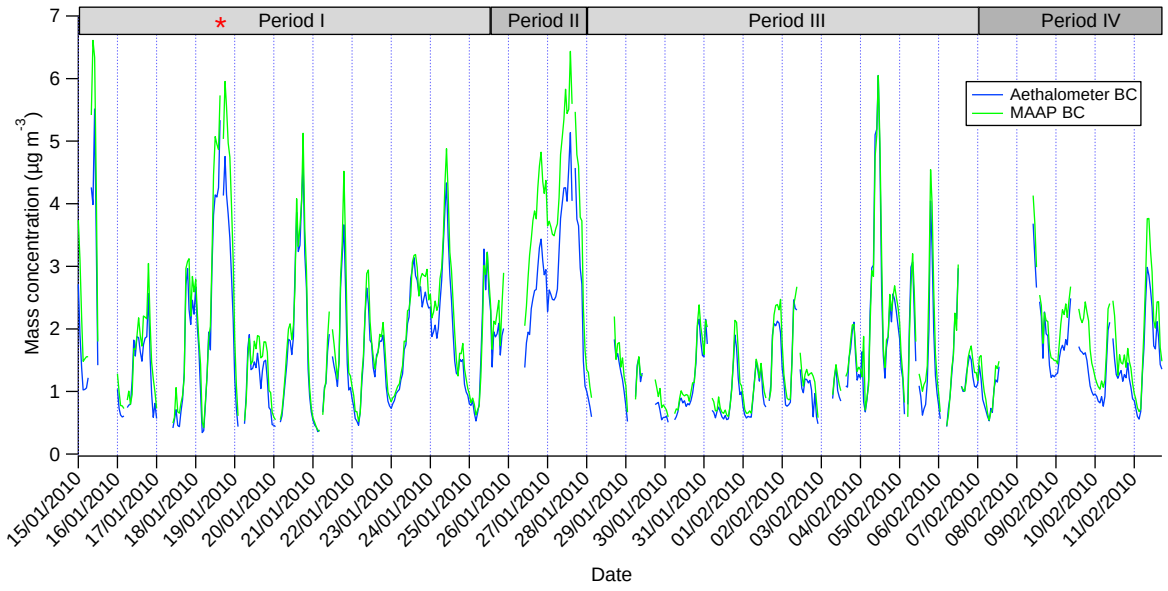

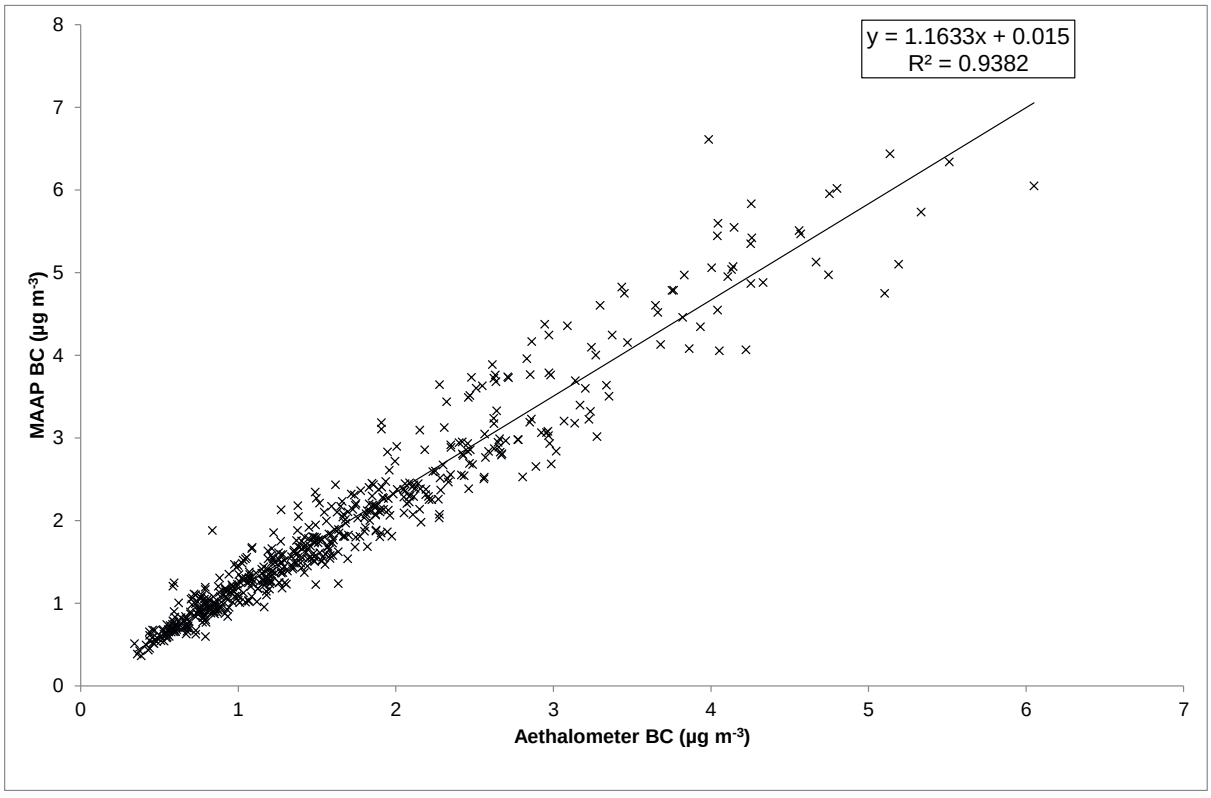

Fig. S10: Comparison of aethalometer BC and MAAP BC

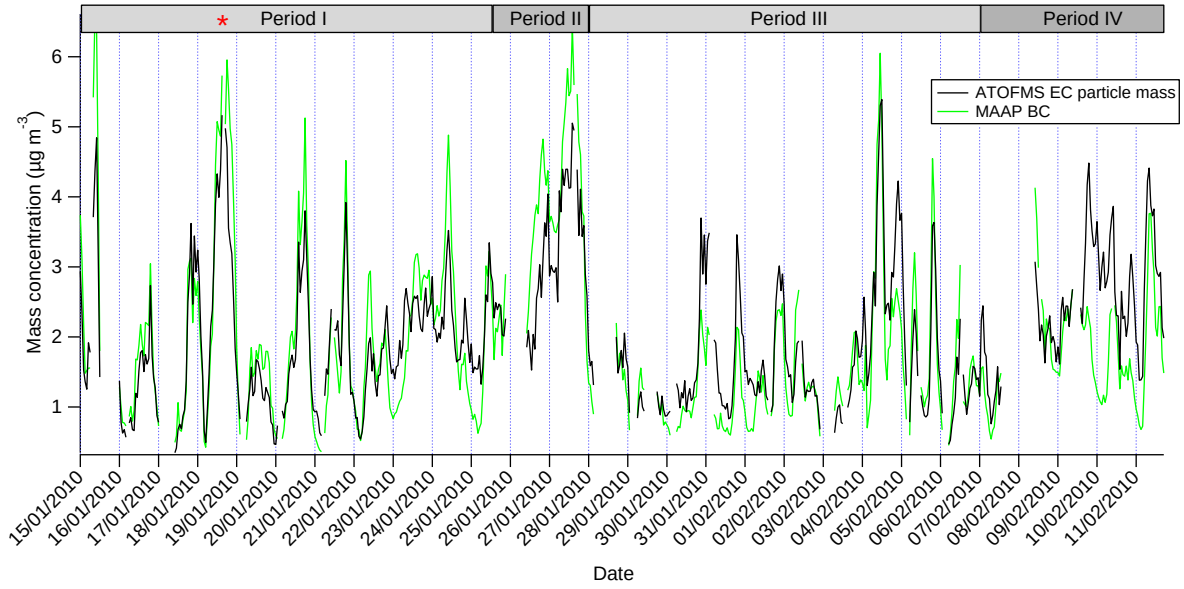

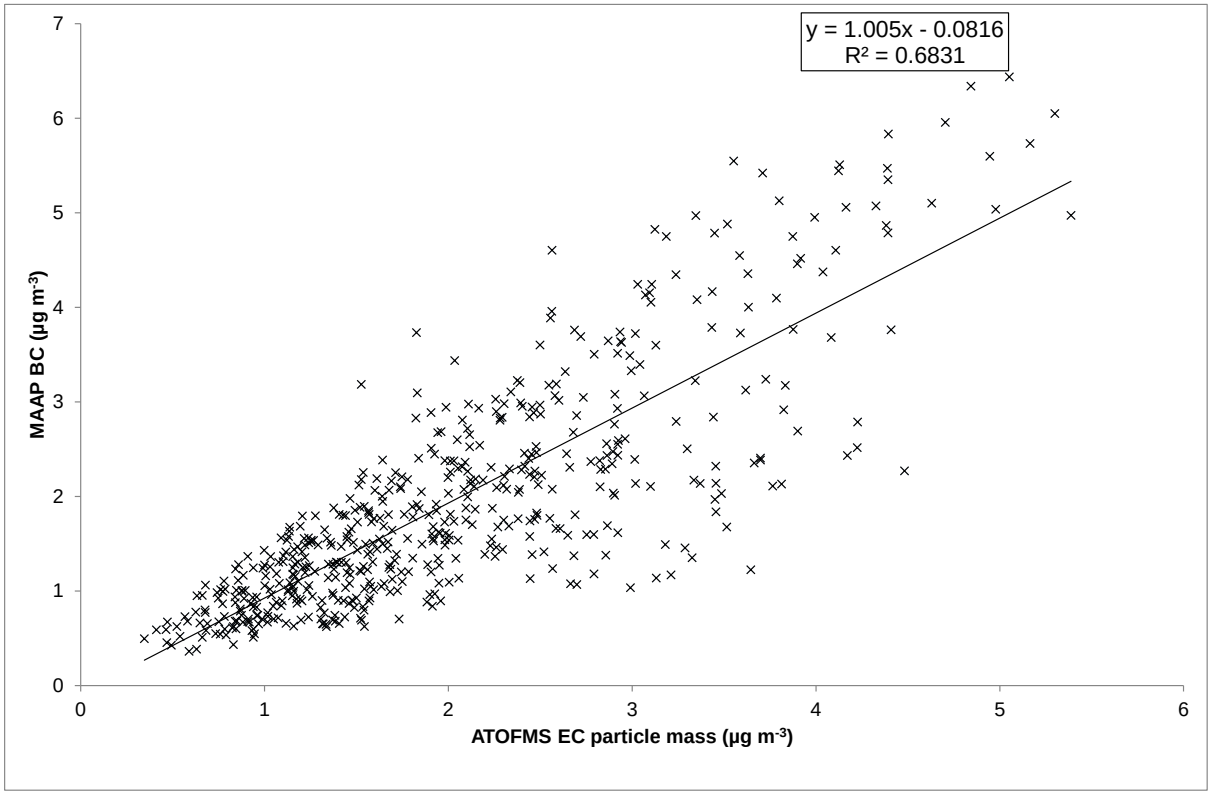

Fig. S11: Comparison of ATOFMS EC particle mass and MAAP BC

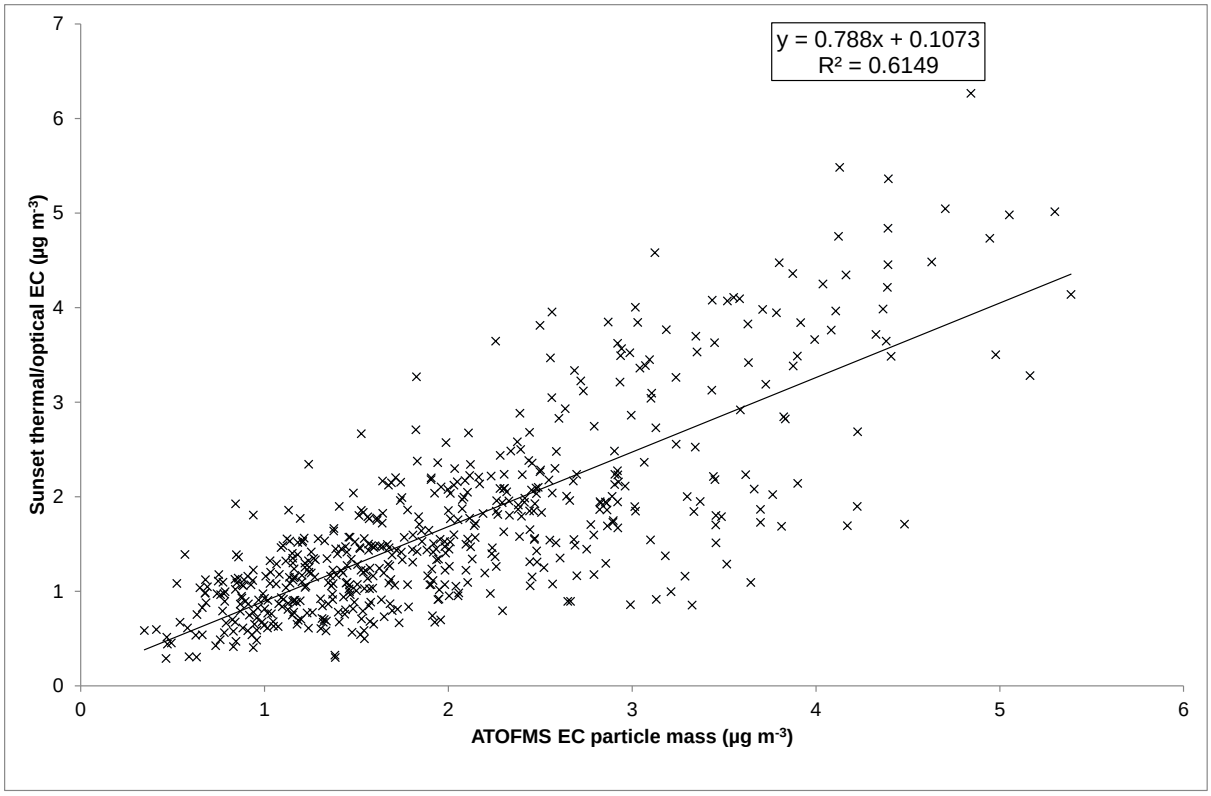

Fig. S12: Comparison of ATOFMS EC particle mass and Sunset thermal/optical EC.

Temporal trends are given in Fig. 7.

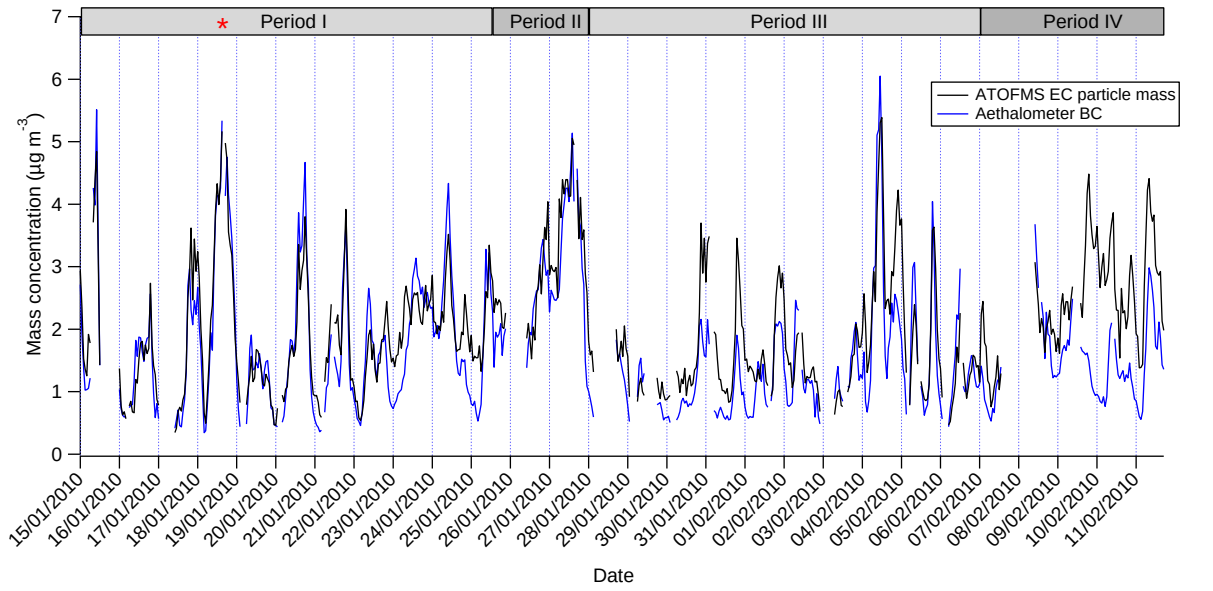

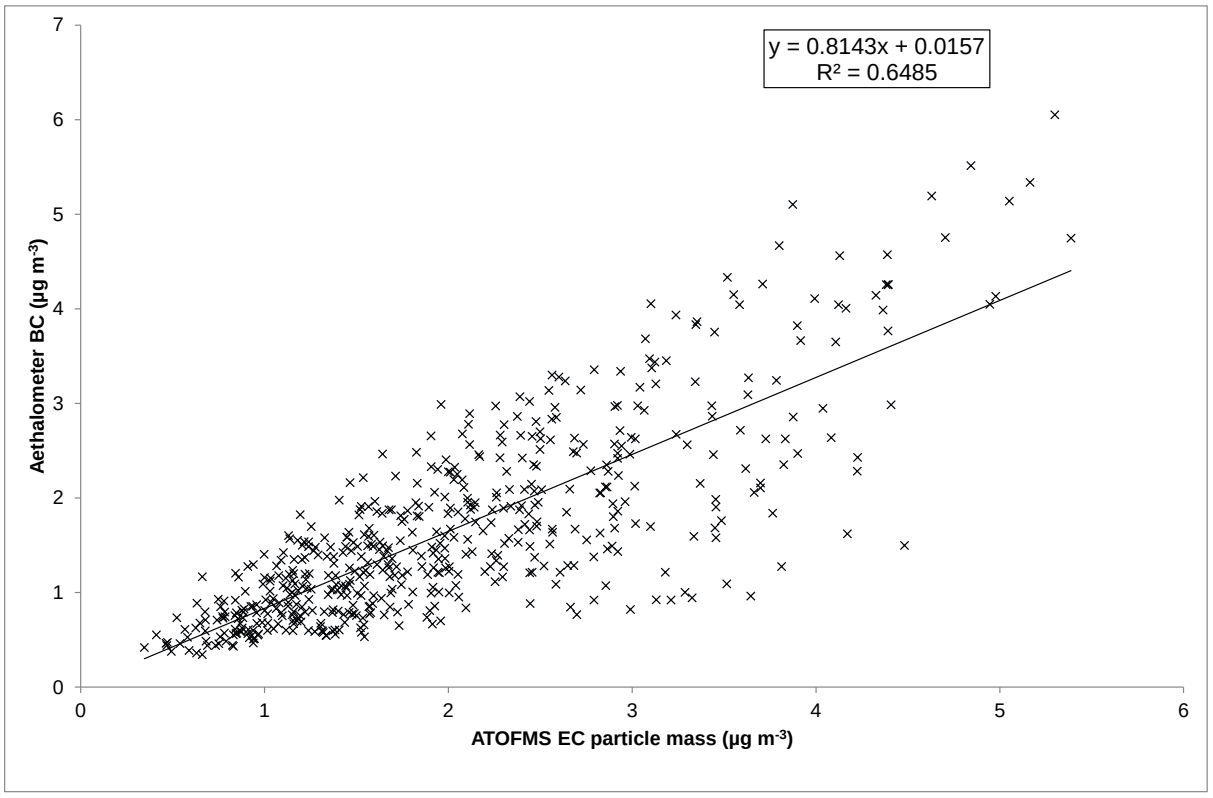

Fig. S13: Comparison of ATOFMS EC particle mass and aethalometer BC

References

Birmili, W., Stratmann, F., and Wiedensohler, A.: Design of a DMA-based size spectrometer for a large particle size range and stable operation, J. Aerosol Sci., 30, 549-553, 1999.

Pratt, K. A., Mayer, J. E., Holecek, J. C., Moffet, R. C., Sanchez, R. O., Rebotier, T. P., Furutani, H., Gonin, M., Fuhrer, K., Su, Y., Guazzotti, S., and Prather, K. A.: Development and Characterization of an Aircraft Aerosol Time-of-Flight Mass Spectrometer, Anal. Chem., 81, 1792-1800, 2009.

Qin, X., Bhave, P. V., and Prather, K. A.: Comparison of Two Methods for Obtaining Quantitative Mass Concentrations from Aerosol Time-of-Flight Mass Spectrometry Measurements, Anal. Chem., 78, 6169-6178, 2006.

Wenzel, R. J., Liu, D.-Y., Edgerton, E. S., and Prather, K. A.: Aerosol time-of-flight mass spectrometry during the Atlanta Supersite Experiment: 2. Scaling procedures, J. Geophys. Res., 108, 8427, 2003.